



HAL
open science

Exploring the integration of bio-based thermal insulations in compressed earth blocks walls

Giada Giuffrida, Laurent Ibos, Abderrahim Boudenne, Hamza Allam

► To cite this version:

Giada Giuffrida, Laurent Ibos, Abderrahim Boudenne, Hamza Allam. Exploring the integration of bio-based thermal insulations in compressed earth blocks walls. *Construction and Building Materials*, 2024, 418, pp.135412. 10.1016/j.conbuildmat.2024.135412 . hal-04715685

HAL Id: hal-04715685

<https://hal.u-pec.fr/hal-04715685v1>

Submitted on 13 Nov 2024

HAL is a multi-disciplinary open access archive for the deposit and dissemination of scientific research documents, whether they are published or not. The documents may come from teaching and research institutions in France or abroad, or from public or private research centers.

L'archive ouverte pluridisciplinaire **HAL**, est destinée au dépôt et à la diffusion de documents scientifiques de niveau recherche, publiés ou non, émanant des établissements d'enseignement et de recherche français ou étrangers, des laboratoires publics ou privés.

Exploring the integration of bio-based insulations for compressed earth blocks walls

Giada Giuffrida^{a*}, Laurent Ibos^a, Abderrahim Boudenne^a, Hamza Allam^a

^a University of Paris Est-Creteil, Certes, Paris, France;

* corresponding author: giada.giuffrida@u-pec.fr

The growing concern about the environmental impact of contemporary construction has posed emphasis on the need of adopting new sustainable building technologies with lower embodied energy, higher energy efficiency and minimized waste production. In this context, bio-based construction and in particular raw earth construction are promising fields that can ensure inexpensive technologies, characterized by wide availability, non-toxicity and high adaptation to several climatic and geographic conditions. The front challenge for the establishment of earth-based technologies in contemporary building markets is the guarantee of high structural and energy performances, which could enable a real competition with conventional building materials which nonetheless have higher environmental impact (clay bricks, concrete masonry units, reinforced concrete).

For this reason, this work focuses on the performance analysis of compressed earth blocks (from now on CEBs) which are currently commercialized for the construction of massive vertical envelopes, with high thermal inertia. However, this is not always sufficient to obtain an acceptable comfort. In fact, it is also necessary to have a construction material with high thermal resistance to optimize thermal behavior.

This issue can be overcome by the design of insulated CEB stratigraphies using bio-based insulations presenting hygrothermal properties compatible with raw earth-based materials. In this way, the thermal performance of CEB walls can be increased so to respond to the high demanding energy standards (recently adopted in several countries), while preserving the hygroscopic behavior of earth-based materials.

In this spirit, this work reports the results of the experimental characterization of the analyzed CEBs combined with two innovative bio-based insulation panels (lime hemp and sugarcane bagasse), comprising their composition, their main physical (dry density, porosity, capillary water absorption), thermal (specific heat capacity, thermal conductivity) and hygrometric (sorption isotherm, water vapor permeability) properties.

Finally, these experimental data are used for the implementation of several numerical simulations at a wall scale in a reference climate to estimate the hygrothermal performances of both uninsulated and bio-insulated CEB walls. The simulations allow for a better comprehension of CEBs' behavior in view of their combination with the chosen bio-based thermal insulations.

Keywords: earth-based construction technologies; compressed earth blocks; bio-based insulation; material characterization; performance analysis.

1. Introduction

The need to adopt new sustainable building technologies with lower embodied energy, higher energy efficiency, and reduced waste production has been highlighted by the growing concern about the environmental impact of the modern construction industry. In this context, bio-based construction and in particular raw earth construction are promising fields which promote the use of low-cost materials, characterized by wide availability, non-toxicity, low tech production processes and recyclability [1]. As highlighted by several works developed during last decades [2], the wide range of earth-based construction technologies show good adaptation to several climatic (hot and temperate climate, but also continental ones) and geographic conditions (seismic-prone areas or not). Promising applications of raw earth technologies explore the possibilities of industrialization, prefabrication, mechanization and digitization [3,4] in response to the need of increasing the reliability, the performances and the streamlining of production and construction processes, without neglecting the cost-effectiveness of the finished product.

Several companies of the construction sector have turned their efforts to the production of contemporary raw earth materials: among these, the pioneering experience of *Cycle Terre* (France) stands out. Indeed, it has set its production of compressed earth blocks and panels, of mortars and earth-based plasters, on the material deriving from the excavations of the *Grand Paris* infrastructure network [5].

Numerous studies focused on the assessment of the performances of compressed earth blocks (CEBs). In the literature, CEBs are often stabilized (for instance with lime and cement) to increase compressive strength, but unstabilized CEBs have proved to reach higher moisture buffer potential and water vapor permeability [6-11]. In [6], unstabilized CEBs store 2.2% of moisture inside them, reach a moisture buffer value of 3 g/(m² %RH), and a water vapor resistance factor of 5.65 on average. In [7], hypercompacted and unstabilized CEB samples have a moisture buffer value of 4.2 g/(m² %RH).

On the other hand, use of stabilizers decreases the capillary water absorption coefficient compared to unstabilized samples [8, 9]. Fiber stabilized CEB materials have in general higher capillary absorption coefficient as shown in

54 [10]. More in general it has been observed that it should exist a threshold value from which an inverse trend (from
55 decrease to increase of capillary water absorption coefficient is recorded [11].
56 In the same work [11], the authors propose a review of the thermal properties of bio-stabilized compressed earth
57 blocks. Because the CEBs analyzed in the present work are unstabilized, we will just recall that the thermal
58 conductivity of unstabilized CEBs' can range from less 0.64 W/mK to 1.46 W/mK, which for this type of raw
59 earth technique, seems to be strictly correlated with the increase of dry density [11].
60 For the reviewed works, dry density ranges between 1600 kg/m³ and 2760 kg/m³. In [12], dry density of CEB is
61 changed to find an optimum between compressive strength and thermal conductivity, by varying the compaction
62 pressure and consequently the porosity. With a minimal compaction pressure of 0.39 MPa, a bulk density of 1610
63 kg/m³ is found, corresponding to a thermal conductivity of 0.618 W/mK; at the same time, for the highest bulk
64 density of 2194 kg/m³, a thermal conductivity of 1.483 W/mK is assessed.
65 Specific heat capacity is a property which is seldom assessed in the literature. In [13], the specific heat capacity of
66 earth brick is assessed to be 869 J/kg K, while in [14] is found a value of 1000 J/kg K. CEB's specific heat capacity
67 was also assessed by [15] where it is found to be equal to 808 J/kg K. Similar values are found for rammed earth
68 materials [17], where specific heat capacity of the unstabilized material is assessed to be equal to 962 J/kg K and
69 in [18] where are reported specific heat capacity above 1000 J/kg K for unstabilized and fiber reinforced rammed
70 earth.
71 Water vapor permeability π and so, water vapor resistance factor μ , of earth materials has been studied in the past.
72 In [19], μ -values varies between 7 and 14 (with the dry cup method) and from 3 to 7 (with the wet cup method).
73 Higher μ -values, up to 14, have been found when stabilizers are used [20], while use of natural fibers in the mix
74 can decrease the water vapor resistance factor [21].
75 In light of these results, it is possible to infer that the high dry density of CEB materials, in combination with the
76 good values of specific heat capacity, entail good inertial properties, beneficial in summer conditions [22].
77 Nonetheless, this is not always sufficient to obtain an acceptable comfort, especially during winter and in more
78 severe climates. In fact, it is also necessary to have a construction material with satisfactory thermal resistance to
79 obtain a satisfactory thermal behavior.
80 This issue can be overcome by the design of insulated CEB stratigraphies which make use of bio-based insulations
81 and are characterized by compatible hygrothermal properties and permeability capacities compared to raw earth-
82 based materials.
83 Only few works have focus on the combination of raw earth walls and thermal insulations. Among them,
84 SIREWALL system, a patented technology used in Canada, proposes a two walls cement stabilized rammed earth
85 with an interior layer of synthetic thermal insulation (as PU or XPS). In [23] the author lists the positive outcomes
86 of using rigid panel insulation interposed between two rammed earth walls; in cold climates, the use of such
87 technology results in mean indoor winter temperatures of 16 °C compared to the 7 °C outside, while humidity is
88 maintained between 40% and 65%, consistent with comfort values. In cold climates, the combined use of thermal
89 insulation (natural or synthetic) and rammed earth walls leads to the amortization of heating consumption by up
90 to 70%, as reported by [24] with reference to four residential buildings in Canada.
91 The same design strategy is adopted in the UK [25]. At first, the authors aimed at designing several retrofit
92 solutions for existing earth based construction systems which could satisfy current UK building standards (with U
93 values below 0.35 W/m²K). They proposed the use of indoor thermal insulations in order not to alter the appearance
94 of the façades and made use of bio-based materials as straw, pads, wool or paper [25]. After that, they developed
95 a new optimized cob construction technology, whose thermal transmittance properties meets current building
96 standards. This wall is done by combining a 30 cm thick loadbearing cob wall (a mix of soil and 2.5% flax straw,
97 with $\lambda = 0.45$ W/mK) with an exterior layer of lightweight thermal insulation (a clay slip with 50% hemp shives
98 and a thermal conductivity of 0.12 W/mK).
99 In [26], the effects of several retrofitting solutions for 14-cm thick CEB walls are studied by means of dynamic
100 thermal simulation in free running conditions on *EnergyPlus* software. The building model is validated by means
101 of measurements made on a real test-box located in a hot and dry tropical country. The work focuses on the impact
102 of type of insulation (synthetic as glass wool, or bio-based as straw and lime) and wall thickness in the enhancement
103 of indoor air temperature profiles. It is found that, in hot and dry climates, uninsulated CEB walls of thickness
104 below 0.35 m are able to perform well without need of thermal insulation; at the same time, a thinner CEB wall
105 (14 cm thick) needs a straw and lime thermal insulation in order to reduce heat conduction through walls until
106 acceptable levels.
107 In general, when used in warm temperate or dry climates, there is a tendency to avoid use of thermal insulation in
108 order to prevent overheating of indoors, even if several authors have pointed out the importance of shading
109 elements and night cross ventilation to prevent from this risk [22, 27]. In continental and cold climates, the need
110 to face low temperatures in winter season has imposed, *de facto*, the use of thick insulation layers on the vertical
111 envelopes. Nonetheless, in Central European Countries as France is, use of hyper insulated envelopes poses serious

112 risks of overheating of indoors in warmer season, especially against a worsening context of rising global average
113 temperatures [28].

114 This work intends to show how using bio-based thermal insulation materials can help in enhancing thermal
115 resistance of CEB walls while preserving the benefices of their thermal mass. Moreover, it is advanced the
116 hypothesis that the combination of hygroscopic materials as raw earth, hemp shives and sugarcane bagasse fibers,
117 determine walls with high permeability toward water vapor, able to store it inside their pores, and favor the
118 humidity buffering effect. Finally, adopting bio-based and local materials as raw earth and hemp, respond to a
119 programmatic sustainable building approach, able to deem with current building regulations as the RE2020, where
120 high energy performances must be accompanied by adequately low environmental embodied carbon values of
121 materials composing future building stock.

122 In order to adapt the performance of raw earth building components to the high energy requirements determined
123 by current regulations, there is an increased need for research works that focus not only on bio-based material
124 performances assessment, but also on their behavior at the masonry scale and at a building scale (even by means
125 of numerical simulations). In this sense, the study of the thermal and hygrometric performances of raw earth walls
126 for exterior walling systems seems fundamental.

127 This work contains the physical, thermal and hygrometric characterization of the compressed earth blocks
128 (currently commercialized by the industrial partner *Cycle Terre*) combined with bio-based insulation materials as
129 lime hemp and sugarcane bagasse. On the base of the material characterization, this paper focuses on the
130 assessment of the hygrothermal behavior of uninsulated and insulated CEB walls by means of numerical
131 simulations. These ones are assessed with *Delphin* software, which allows investigating the building components
132 behavior under combined heat, moisture, air, and salt transport. In a second phase of the research, the uninsulated
133 and bio-based insulated CEB walls constructions are further studied by means of wall scale measurements in a Hot
134 Guarded Box Equipment.

135 **2. Materials**

136 **2.1 Compressed earth block (CEB)**

137 The compressed earth blocks provided by *Cycle Terre* are designed for several applications, including load-bearing
138 walls (for single-story or double-story buildings), being their compressive strength at least 2.00 MPa, but also
139 massive walls applications in combination with load-bearing framing and curtain walls. The CEBs are realized in
140 different sizes depending on the application, but all of them use a mix design made up of at least 65% of raw earth
141 (composed by clays, silts, sands and small gravels) and 35% sand (with a particle size distribution comprised
142 between 0 and 2 mm or from 0 to 4 mm) from Paris region [29]. CEBs are sold in various sizes, but the more
143 common is the block with dimensions 9.5 x 15 x 31.5 cm, that weighs 8.7 kg. The environmental performance of
144 30 cm thick CEB walls has been calculated by the company and it has been found a global warming potential of
145 27.8 kg eq. CO₂ for the production phase of 1 m² functional unit.

146 **2.2 Lime hemp (LH)**

147 Lime-hemp or hempcrete is a biomass-based product, which is currently used for non-load-bearing purposes in
148 new construction to produce blocks for walling systems, but also for roof insulation. Moreover, it is increasingly
149 used for the energy retrofit of existing building stock. The use of hemp shives and lime or cement leads to insulating
150 mixes with really low dry density (ranging from 200 kg/m³ to 800 kg/m³) and thermal conductivity (ranging from
151 0.06 W/m K to 0.18 W/m K) [30]. These types of walls present thermal resistance from 0.22 K m²/W to 0.40 K
152 m²/W from low to medium density (200 – 400 kg/m³). Lime hemp or hempcrete materials have also high specific
153 heat capacity, being it around 1500 J/kg K in the dry state and up to 2900 J/kg K at 99% RH [31]. As raw earth,
154 lime hemp and hempcrete mixes are known to be able to regulate relative humidity. It has been found to have a
155 water vapor permeability of 2.3 10⁻¹¹ kg/Pa m s, and a moisture buffer value (the ability of a material to uptake or
156 release moisture when it is exposed to repeatedly varying levels of relative humidity) of 2 g/m² %RH [32, 33].
157 Water vapor resistance coefficient of hemp concrete was assessed in [34] and it was found to be ranging between
158 1.49 and 2.30 depending on the calculation method, while in [35] it was found a μ -value ranging from 5.42 to 5.71
159 depending on the concrete type.



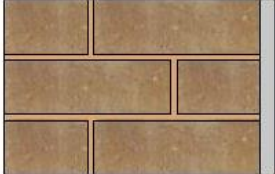
160 **2.3 Sugarcane bagasse (SB)**

161 Sugarcane, scientifically known as *Saccharum officinarum*, is a tall grass plant with strong stems, largely grown
 162 in Southeast Asia, South American and South Africa [36]. Sugarcane bagasse is an agro waste, a byproduct
 163 obtained after extraction of the juice from sugarcane stalks.
 164 Various studies [36, 37] reported that its chemical composition is composed by cellulose, hemicellulose, lignin.
 165 The cellulose content of sugarcane bagasse helps to reduce the use of synthetic binders. Considering the abundance
 166 of sugarcane bagasse, it is currently investigated as an ideal raw material to produce low-cost green thermal
 167 insulation which could also satisfies environmental regulations, given its biodegradability and reusability.
 168 Previous studies found that sugarcane bagasse insulation materials exhibited low thermal conductivity 0.034–
 169 0.0496 W/m K for densities ranging from 100 kg/m³ to 200 kg/m³ and porosity from 83.33% to 92.18% [36]. The
 170 company *Emerwall* provided the sugarcane bagasse panels characterized in this study.
 171

172 **2.4 Design of insulated and bio-based insulated CEB constructions**




173 Several raw earth standards indicate the minimum thicknesses of CEB walls for structural stability to be within
 174 0.3 and 0.4 m [38, 39]. The new CEB French standard does not indicate minimal thickness, but the ATEX provided
 175 by the company *Cycle Terre*, indicates possible combinations of not loadbearing CEB envelopes with several
 176 loadbearing frames in wood or concrete. The BTC masonry is framed by stiffeners (integrated into the main
 177 structure of the building or not) whose maximum spacing depends on the thickness, on the height of the masonry
 178 and on its exposure to the wind. In particular, the ATEX presents the possibility of realizing 0.15 m thick CEB
 179 walls coupled with an eventual thermal insulation and a wood ventilated façade, or thinner CEB walls, 0.095 m
 180 thick, coupled with a mandatory thermal insulation. It also specifies that the thermal resistance of CEB walls must
 181 be adequate to the local climate and energy performances standard requirements.
 182 In this work CEB wall thicknesses of 0.15 m, 0.30 m and 0.45 m have been studied in order to estimate the change
 183 in hygrothermal behavior of uninsulated and bio-insulated CEB walls depending on raw earth wall thickness.
 184 Moreover, several bio-based insulations have been considered, namely lime hemp and sugarcane bagasse
 185 insulations, with several thicknesses which enable the achievement of a range of thermal transmittances and
 186 allowing for the adoption of CEB walls in a wide assortment of climatic conditions. The insulation layers are
 187 always applied to the outmost layer of CEB walls in order to take advantage of the thermal inertia of the raw earth
 188 wall, according to what has been found in previous research [22, 26, 40]. In table 1, 2, 3 are reported the main wall
 189 scenarios considered in the simulation study explained section 3.

Table 1. Scenarios of CEB wall thicknesses

	CEB 15 0,15 0,025	CEB 30 0,3 0,025	CEB 45 0,45 0,025
			
INNER SIDE	0.15 m thick CEB wall	0.30 m thick CEB wall	0.45 m thick CEB wall
OUTER SIDE	0.025 m Lime Plaster	0.025 m Lime Plaster	0.025 m Lime Plaster

190




Table 2. Scenarios of CEB walls insulated with an outside lime hemp (LH) insulation

	LH 5 0,3 0,05 0,025	LH 10 0,3 0,1 0,025	LH 15 0,3 0,15 0,025
			
INNER SIDE	0.30 m thick CEB wall	0.30 m thick CEB wall	0.30 m thick CEB wall

	0.05 m Lime Hemp	0.10 m Lime Hemp	0.15 m Lime Hemp
OUTER SIDE	0.025 m Lime Plaster	0.025 m Lime Plaster	0.025 m Lime Plaster

191

Table 3. Scenarios of CEB walls insulated with an outside sugarcane bagasse (SB) insulation

	SB 5	SB 10	SB 15
	0,3 0,05 0,025	0,3 0,1 0,025	0,3 0,15 0,025
			
INNER SIDE	0.30 m thick CEB wall	0.30 m thick CEB wall	0.30 m thick CEB wall
	0.05 m Sugarcane Bagasse	0.10 m Sugarcane Bagasse	0.15 m Sugarcane Bagasse
OUTER SIDE	0.025 m Lime Plaster	0.025 m Lime Plaster	0.025 m Lime Plaster

192

193

194

195

196

3. Methods

3.1 Material characterization

197

198

199

200

201

202

203

204

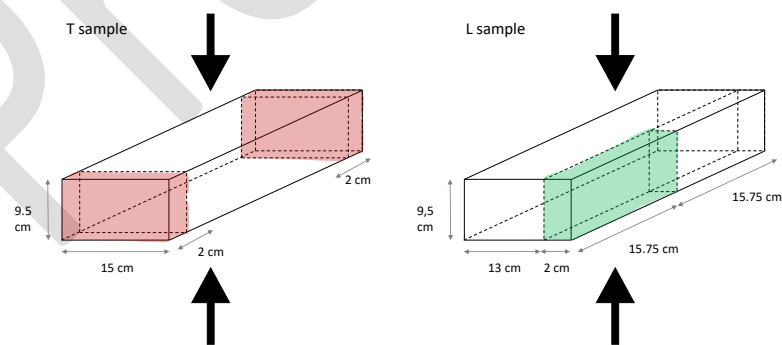
205

206

207

208

A material characterization campaign was carried out on the three main innovative materials at the center of this study: compressed earth blocks (CEB), lime hemp (LH) and sugarcane bagasse (SB) thermal insulations. The characterization comprises the assessment of the main physical (dry density, porosity, capillary water absorption), thermal (specific heat capacity, thermal conductivity) and hygrometric (sorption isotherm, water vapor permeability) properties. Please note that the porosity of CEB samples is assessed for two portions of material: one taken from the surface and the other from the core of the CEB block. Besides, the thermal conductivity of CEB blocks is measured in two main directions, corresponding to samples cut in the longitudinal and transversal direction of the entire compressed earth block. This choice was motivated by the fact that in a double layer CEB wall (as for instance are the CEB 30 and CEB 45 wall configurations of the present study), CEBs are arranged in both directions, and an eventual inhomogeneity of thermal conductivity performance in the two directions would have caused an effect on the final wall behavior. Figure 1 shows the two cuts of CEB samples and the direction of compaction they are produced with.



209

210

Figure 1. Cut directions for T and L CEB samples

211

3.1.1 Dry density

212

213

214

215

Dry density was assessed after oven-drying three samples of each materials at 70 °C (about 7% RH) to constant weight until steady state was reached (namely, two measures 24 hours apart differ of less than 0.1% $m_{(t,t+24)} < 0.1\%$). After oven-drying, samples were weighted and their mass divided for the volume (sizes of samples were asessed via a caliper).

216

3.1.2 Porosity

217 Mercury intrusion porosimetry (MIP) is a method used to determine the dimensions of the pores in a material and
 218 their distribution. A non-wetting liquid (mercury) is forced into the material's pores by external pressure, until it
 219 reaches the smallest pores. Being the volume of intruded liquid known, it is possible to assess the pore size
 220 distribution at each pressure increment. This method is used to measure the range of pores between 0.0025 μm
 221 and 430 μm . For the analysis, an AutoPore IV 9500 V1.10 porosimeter from Micromeritics Instrument Corporation
 222 was used, capable of applying pressures up to 207 MPa. The contact angle between the solid and the mercury was
 223 assumed to be 140°, with a surface tension of 0.485 N/m. The quantity investigated for a typical experiment was
 224 around 1.2 g per sample for compressed earth block samples and 0.13 g for the bagasse insulation.
 225 The total volume porosity in water method was instead used to estimate porosity inside the lime-hemp insulation
 226 [41, 42]. The total volume porosity can be calculated in the water by measuring the block weight after water
 227 saturation from the initial dry weight, because of the absorbed water by the block which penetrates into accessible
 228 pores in the block. The volume of water absorbed to saturation is equal to the total volume of the block pores.
 229 Thus, the total water absorption is converted to porosity using the following:

$$230 \quad n(\%) = \frac{TWA * \rho}{100 * \rho_w}$$

231 $n(\%)$ = total volume porosity.

232 ρ = block dry density (kg/m^3)

233 ρ_w = water density 1000 (kg/m^3).

234 TWA= total water absorption (%).

235 *3.1.3 Capillary water absorption and free water saturation*

236 The water absorption coefficient A_w due to capillary action is determined for three samples of each material by
 237 partial immersion according to the standard NF EN ISO 15148:2003. Oven-dried samples (at 70 °C until mass
 238 stabilization $m(t, t + 24) < 0.1\%$) are thus brought into contact with the 5 mm water level and left to soak for an
 239 appropriate time. The samples are removed from the water and weighed at preset time intervals. The results are
 240 expressed as the ratio of mass change to base area and then plotted against the square root of time to calculate the
 241 water absorption coefficient. The test was easily run for the two insulation materials (LH and SB), taking care of
 242 letting the material drain all the free water contained in their open pores, by gravity action. On the other hand,
 243 considering the extreme affinity of the unstabilized CEBs with water, in this study the contact with water was
 244 mediated by means of a perforated basket equipped with absorbent paper, so that the water could pass through
 245 without causing any loss of material in the water. Mass increase of absorbent paper was deducted from separate
 246 measurements. Similar approaches have been used previously in the literature, where the contact of the unstabilized
 247 block with water was mediated, for example, by a wet sponge or sand [43, 44]. Once the test was completed, the
 248 free water saturation of the materials was assessed by immersing the samples inside water. The samples were then
 249 kept in water until the weight was stabilized with a mass variation of 0.1%. In particular, CEB samples were closed
 250 in absorbent paper to allow water saturation thus avoiding any loss of material during the test.

251 *3.1.4 Moisture dependent thermal conductivity and specific heat capacity*

252 Moisture dependent thermal conductivity was assessed on 2 cm-thick CEB and 4 cm-thick LH and SB samples.
 253 Samples were left in a climatic chamber at a constant temperature of $T = 20^\circ\text{C}$, while relative humidity was
 254 successively increased following the methodology already adopted in [18, 45]. Thermal conductivity was assessed
 255 on several points of sample's surface and when its mass was stabilized: more in detail, a condition of mass
 256 stabilization $m(t, t + 24) < 0.1\%$ was adopted because of the need of adopting bigger sizes of samples due to
 257 minimal thermal conductivity measurement area. The relative humidity steps were 25% RH, 40% RH, 60% RH,
 258 80% RH.

259 The samples were kept in the climatic chamber during the thermal conductivity measurements with a Hot Disk
 260 device (NF EN ISO 22007-2), a transient method using a flat probe that serves as both a heating device and a
 261 temperature sensor. The probe is placed between two identical, smooth, flat samples to avoid contact with air. This
 262 measurement method allows the determination of thermal conductivity and heat capacity for any water content,
 263 with a fast and reliable procedure. A Kapton 5501 probe with a radius of 6.403 mm, a power of 90 mW and a
 264 measurement time of 80 s was used for the measurement of CEB thermal conductivity. A Kapton 8563 probe with
 265 a radius of 9.868 mm was used both for LH and SB samples, with a measurement time of 80s and a power of
 266 33mW for LH and 30mW for SB.

267 The same Hot Disk measurements and parameters were used for specific heat capacity assessment. In this case
 268 only dry state specific heat capacity was determined, by previously oven drying samples at 25°C until mass
 269 stabilization ($m(t, t + 24) < 0.1\%$).

270 3.1.5 Sorption isotherms

271 The sorption isotherm is assessed in accordance with NF EN ISO 12751:2021; in particular, the sorption step
 272 consists of successively placing a previously dried sample (at 70°C until stabilization of the mass $m(t, t + 24) <$
 273 0.1%), in several environments with increasing relative humidity and constant temperature. In this work, three
 274 samples of each material (CEB, LH and SB) were put in a climatic chamber with a temperature of 23°C and a
 275 ventilation rate of 100%, and increasing relative humidity of 25% RH, 40% RH, 60% RH, 80% RH. Moreover, a
 276 further sorption condition, equal to 95%RH, was reached inside a desiccator and using a saturated salt solution of
 277 Na_2PHO_4 . The sample is weighed periodically, and it remains in a given environment until a constant mass ($m(t,$
 278 $t + 24) < 0.01\%$) is obtained. Then, the percentage of mass increase due to moisture penetration is calculated.

279 3.1.6 Water vapor permeability

280 Water vapor permeability is commonly assessed according to the "wet cup" or "dry cup" methods using the
 281 standard EN ISO 12572. The experimental protocol used for these two tests consists in sealing the samples on a
 282 "wet" or "dry" cup whose relative humidity is controlled by a saturated salt solution. These cups are then placed
 283 in a climatic chamber (with controlled T and RH), so that the tested material is located between two environments
 284 with different vapor partial pressures, namely and outside p_{v1} and an inside (cup) p_{v2} . It is important to remark
 285 that a layer of air is present inside the cup. The partial vapor pressure gradient between the inner part of the cup
 286 and the outside (the climatic chamber), enables a flow of water vapor through the sample: in particular, during the
 287 dry cup test the assembly of the cup and the sample experiences a mass uptake, while during the wet cup test the
 288 assembly experiences a mass loss.

289 For the wet cup, a di-sodium hydrogen phosphate solution is used, leading to a relative humidity level of 95% at
 290 23°C. For the dry cup, potassium hydroxide solution (RH level, 8% at 23°C) was used. To seal the samples to the
 291 cup, silicon and vapor-tight aluminum tape are used, because they do not adsorb a significant quantity of moisture
 292 themselves. Tested samples (CEB, LH, SB) have all a minimum surface of 10 cm². Two samples were tested for
 293 each condition, being previously dried in an oven at 70°C until mass was constant ($m(t, t + 24) < 0.1\%$). The cup
 294 systems are then put in a chamber at 50%RH and 23°C, and their mass evolution is assessed every 24 hours until
 295 steady-state is reached.

296 In particular, the mass change rate Δm_{12} is calculated as the ratio between the difference of masses (measured in
 297 kg) of the test assembly at time t_2 and t_1 , and the times of weighing themselves (measured in seconds). G is the
 298 mean of five successive determinations of Δm_{12} . Equilibrium is attained when each of the last five successive
 299 determinations of Δm_{12} is within a variation of 5% of G value.

300 After that, it is calculated the density of water vapor flow rate g , as the ratio between G and the exposed area A of
 301 the specimen (in m²). The G value is used to calculate the water vapor permeance W , by this formula:

$$302 \quad W = \frac{G}{A \Delta p_v}$$

303 where Δp is the difference in partial pressure of vapor between the two faces of the samples, which can be
 304 calculated as [46]:
 305

$$306 \quad p_v = RH * \exp\left(23.5771 - \frac{4042.9}{T - 37.58}\right)$$

307
 308 The water vapor resistance Z is the reciprocal of the water vapor permeance W . From W value it is possible to
 309 calculate the water vapor permeability by multiplying it for the sample thickness:

$$310 \quad \delta = Wd$$

311 Assuming that inside the cup there is an ideal mixing of humid air, the water vapor resistance factor μ is:

$$312 \quad \mu = \frac{Sd_{tot} - d_{air}}{d}$$

313 where d_{air} is the thickness of air layer between the sample and the saturated salt solution in the cup and Sd_{tot} is the
314 total vapor diffusion thickness:

$$315 \quad Sd_{tot} = \frac{\delta_{air} A \Delta p_v}{G}$$

316 Where δ_{air} is the water vapor permeability of air, that is calculated as:

$$317 \quad \delta_{air} = 2.306 \cdot 10^{-5} \frac{M_w}{RT} \left(\frac{T}{273.15} \right)^{1.81}$$

318 With $R = 8.314$ [J mol⁻¹ K⁻¹] is the ideal gas constant, $M_w = 18$ [g mol⁻¹] the molar weight of water.

319 **3.2 Walls behavior : Hygrothermal performance simulation**

320 In this study, material properties assessed for both CEBs and bio-based thermal insulations (SB, LH) are used to
321 run several numerical simulations in order to assess the hygrothermal behavior of both uninsulated and bio-based
322 insulated CEB walls. Several design solutions (introduced in paragraph 2.4), are simulated by means of the
323 software tool *Delphin 6.1.2*. This software allows for the numerical solving of balance equations in a finite control
324 volume to describe the combined heat and mass transfer inside the wall construction. For each investigated
325 material, the software requires several hygrothermal properties to describe the following functions:

- 326 • heat transfer and heat storage (for which are implemented bulk density ρ , specific heat capacity c_p and
327 dry thermal conductivity λ);
- 328 • moisture storage (for which sorption isotherm are required, not taking in consideration the desorption
329 phase and the eventual hysteresis);
- 330 • vapor transport (quantified by water vapor resistance factor μ);
- 331 • liquid water transport (described by the capillary water absorption coefficient A_w).

332 In this study, hygrothermal simulations are run in the reference climate of Paris (France) classified as a Cfb (marine
333 west coast climate), and performed over three consecutive years, with initial conditions $T=25^\circ\text{C}$ and $\text{RH}=60\%$ for
334 all the materials.

335 The target objectives of this study are the estimation of average (1) temperature distribution and (2) moisture
336 contained in the walls, with particular reference to the change in moisture contained in CEB wall when a bio-based
337 thermal insulation is added. The study also envisages the assessment of (3) moisture dependent thermal
338 transmittance, whose fluctuation could cause an increase of heat losses through the envelope, by calculating it on
339 the base of the moisture dependent thermal conductivity values assessed by simulation for each material used [47].
340 The simulation study investigates the influence of CEB walls and thermal insulation thicknesses in the (4) dynamic
341 wall behavior with attention to summer conditions for the estimation of dynamic parameters as decrement factor
342 and time lag. Time lag is the time delay required for the heat wave to be transferred from one side to the other of
343 a wall. It is calculated by the following equation:

$$344 \quad \text{TL} = t_{T_{si, \max}} - t_{T_{so, \max}}$$

345 Decrement factor is the ratio of the heat wave amplitude on the inner and outer surface of the wall and it is
346 calculated with the following equation:

$$347 \quad \text{DF} = \frac{T_{si, \max} - T_{si, \min}}{T_{so, \max} - T_{so, \min}}$$

348 **4. Results and discussion**

349 **4.1 Materials' properties**

350 **4.1.1 Physical properties**

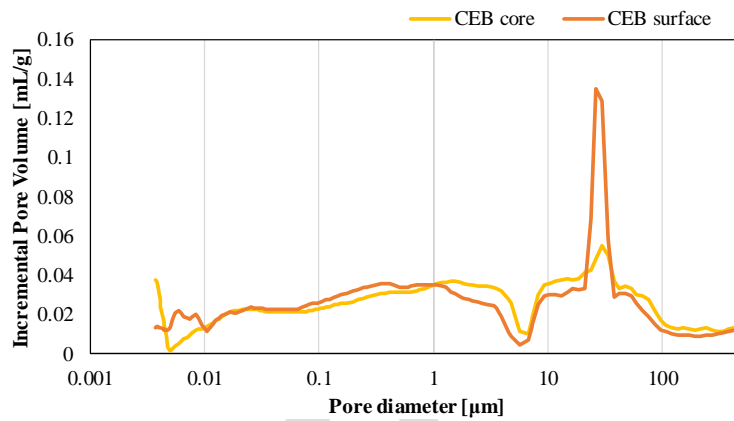
351 In table 3 are reported the main physical properties assessed for the three investigated materials. Dry density
352 average value for CEB is around 1800 kg/m^3 , according to the values reported in the manufacturer data sheet.
353 Concerning SB and LH thermal insulations, the assessed values are respectively 54.6 kg/m^3 and 394.8 kg/m^3 .
354 The porosity values are 24.3% for the CEB core sample, 24.9 for the CEB surface sample, 74% for the SB
355 (calculated by means of MIP), and 55% for LH (calculated with TWA method). Figure 2 show the pore diameter

356 against the incremental pore volume for compressed earth blocks samples, which allow for a deeper
 357 comprehension of the pore distributions inside the material, and reveals the difference in pore distribution between
 358 CEB core and surface samples.
 359 The dry density values for *Cycle Terre* CEB is in the average compared to what is found in the literature. Indeed,
 360 the relatively low dry density is accompanied by a low porosity, even when compared with other CEBs tested [12,
 361 45], for which the porosity values are around 30%. The porosity of SB sample found in this study is lower
 362 compared to values reported in [34].

363 *Table 4. Physical properties of materials analyzed in this study*

	CEB	LH	SB
Dry density [kg/m ³]	1800	394.8	54.6
Porosity [%]	24.3 (core) – 24.9 (surface)	55	74
Capillary water absorption coeff. [kg/m ² s ^{1/2}]	0.137	0.112	0.113

364



365

366 *Figure 2. Mercury Intrusion Porosimetry for CEB core and surface samples*

367 Figure 3 shows the setup adopted for the capillary water absorption test of CEB samples. The capillary water
 368 absorption coefficient A_w of CEB sample is found to be equal to 0.137 kg/m²s^{1/2}, while the A_w 0.113 and 0.112 for
 369 SB and LH respectively. The capillary water absorption of the CEB at 24 hours is lower compared to values found
 370 in [8, 9], fact which is easily explained by the reduced percentage of porosity compared to other CEBs analyzed
 371 in the literature.

372 Once the test is completed, samples were totally immersed inside water to assess water content at saturation. In
 373 particular, CEB samples were transferred inside absorbent paper bags and brought at saturation.



Figure 3. Capillary water absorption test for CEB samples

4.1.2 Thermal Properties

Table 5 show the thermal properties assessed for the CEB sample cut in the longitudinal direction (CEB L) and for the one cut in the transversal direction (CEB T) of the blocks. The thermal conductivity values for the CEB L samples range from 0.833 W/m K at 25%RH to 0.903 W/m K at 80%RH. For the CEB T samples the values are higher and range from 0.980 W/m K at 25%RH to 1.021 W/m K at 80%RH.

It is important to point out that the slight difference between thermal conductivity values for the two samples cut in the longitudinal and transversal direction may be due to the specific manufacturing procedure adopted, using a double compression on the upper and lower surface of the CEB. This process could likely make the extremities of the CEBs more compacted compared to the lateral samples.

The porosity of CEB samples enables the storage of moisture within the material when ambient relative humidity increases. In this condition, the thermal conductivity of samples increase because moisture contained in the sample leads to heat transfer by conduction.

Noticeably, the obtained thermal conductivity values are lower compared to other CEBs' thermal conductivity values with similar density [12, 45], even if the porosity of *Cycle Terre* CEBs is lower. This apparent contradiction can be explained by the fact that the analyzed CEBs have an optimized particle size distribution (leaving less pore) and use solid phase components with a considerable lower conductivity.

Table 5. Thermal conductivity of CEB blocks in two different directions

	CEB L	CEB T
$\lambda_{25\%RH}$ [W/m K]	0.833 ± 0.0002	0.980 ± 0.0003
$\lambda_{40\%RH}$ [W/m K]	0.868 ± 0.0009	0.985 ± 0.0007
$\lambda_{60\%RH}$ [W/m K]	0.875 ± 0.0024	0.996 ± 0.0015
$\lambda_{80\%RH}$ [W/m K]	0.903 ± 0.0020	1.021 ± 0.0021

The good thermal insulating properties of the SB and the LH are confirmed by the thermal conductivity values reported in table 6. In particular, LH insulation values range from 0.115 to 0.13 W/m K, while SB insulation have thermal conductivity values which vary from 0.049 to 0.059 W/m K, for relative humidity values ranging from 25%RH and 80% RH.

The dry thermal conductivity of lime-hemp insulation assessed in this study is an average value compared to those reported in [30]. The few studies conducted on sugarcane bagasse insulation confirm the data found in this study. Indeed, for a low-density sugarcane bagasse panel, it is found a thermal conductivity of 0.049 at the dry state and of 0.095 at the moist state [34].

403

Table 6. Thermal conductivity of analyzed thermal insulating materials

	LH	SB
$\lambda_{25\%RH}$ [W/m K]	0.115 ± 0.0017	0.049 ± 0.0001
$\lambda_{40\%RH}$ [W/m K]	0.116 ± 0.0018	0.051 ± 0.0003
$\lambda_{60\%RH}$ [W/m K]	0.120 ± 0.0013	0.054 ± 0.0001
$\lambda_{80\%RH}$ [W/m K]	0.131 ± 0.0008	0.059 ± 0.0002

404

405 The specific heat capacity of samples (reported in table 7) was assessed in dry conditions, at 20°C and 25%RH for
 406 all the tested samples. CEB samples have specific heat capacity about 816.11 J/ kg K, while SB samples have a c_p
 407 value of 1438 J/ kg K and LH samples of 495.46 J/ kg K.

408 The specific heat capacity of the studied CEBs is slightly lower compared to other studies [13, 14, 16, 17],
 409 nevertheless it is worth to remind that this value is obtained without use of binders or fibers integrated in the mix,
 410 as it is often done in the literature. Specific heat capacity value for the LH sample is slightly lower compared to
 411 [31], probably because of the absence of sand in the lime hemp mixture used in present study.

412

Table 7. Dry weight Specific Heat Capacity

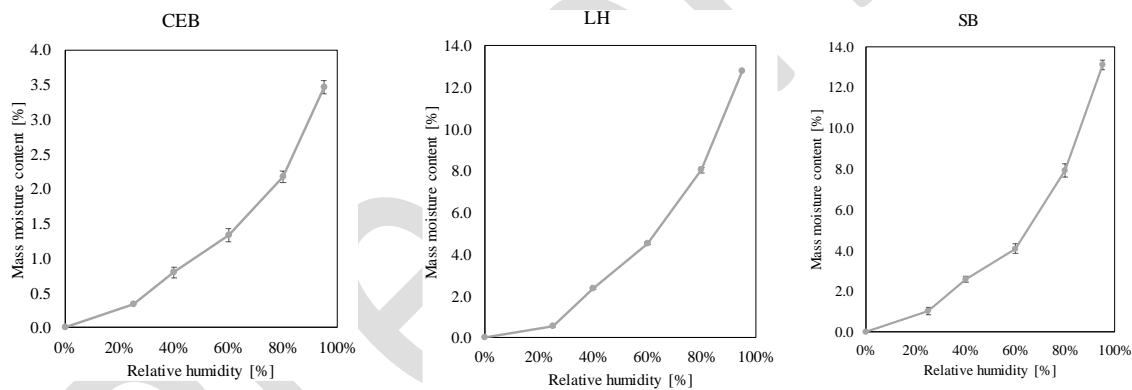
	CEB	LH	SB
$c_{p\ DRY}$ [J/ kg K]	816.11 ± 30.508	495.46 ± 6.918	1438 ± 24.464

413

414

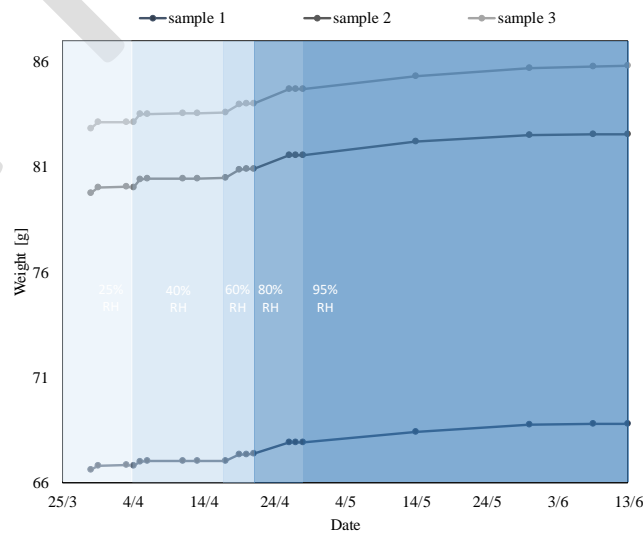
4.1.3 Hygric properties

415 Sorption isotherms for all the investigated materials were assessed and are shown in figure 4. Moreover, an
 416 example of the kinetic of sorption of CEBs is shown in figure 5.



417

Figure 4. Sorption curves of the analyzed material



418

419

Figure 5. Evolution of mass moisture content in increasing relative humidity for CEB samples

420 It is important to point out that the first part of the sorption curve (until a relative humidity of 80%) was performed
 421 inside a climatic chamber with a ventilation system activated. Instead, the 95% relative humidity condition was
 422 performed inside a desiccator, without any ventilation, which made the sorption process in the last step much
 423 slower.

424 For Delphin simulation it is important to know quantify the water content at 80%RH (the well-known W80 value),
 425 which is found to be equal to 39.705 kg/m³ for the CEB, 9E-06 kg/m³ for the SB sample and 33.603 kg/m³ for the
 426 LH sample. The W80 of CEB entails good moisture storage properties.

427 Concerning the water vapor permeability test, the following values (table 8) were assessed.

428 *Table 8. Water vapor permeability and water vapor diffusion resistance factor of the material*

Test	Sample	CEB	LH	SB
Dry cup	δ [kg/m s Pa] 10 ⁻¹¹	2.18	5.39	1.37
	μ [-]	8.87	3.65	1.41
Wet cup	δ [kg/m s Pa] 10 ⁻¹¹	3.93	6.74	1.61
	μ [-]	4.92	2.91	1.20

429 When comparing these results with values from the literature, the water vapor permeability of CEB measured in
 430 this study is higher compared to other raw earth products [19]; besides, the water vapor resistance factor obtained
 431 for the lime hemp insulation is comparable with other works as [34, 35].

432 Material properties of CEB, LH and SB assessed in this study are resume and reported in table 9.

433

434 *Table 9. Resume of material properties obtained in this study*

	Dry density	Porosity	Capillary water absorption	Thermal conductivity (RH)	Specific heat capacity	W80	Water vapour res. factor
	[kg/m ³]	[%]	[kg/m ² s ^{1/2}]	[W/mK]	[J/kgK]	[kg/m ³]	[-]
CEB	1800	24.3 (core)	0.137	0.833 - 0.903	816.11	39.705	8.87
		24.9 (surface)		0.980 - 1.021			(dry cup)
LH	394.8	55	0.112	0.115 – 0.131	495.46	36.002	4.92
							(wet cup)
SB	54.6	74	0.113	0.049 - 0.059	1438	9.00E-06	3.65
							(dry cup)
							2.91
							(wet cup)
							1.41
							(dry cup)
							1.20
							(wet cup)

435

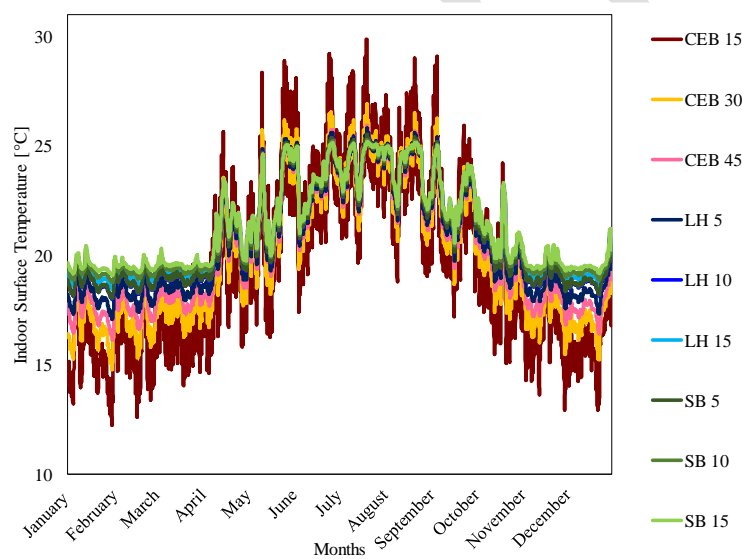
436 **4.2 Hygrothermal walls behavior**

437

438 *4.2.1 Temperature distribution and dynamic walls behavior*

439 Ensuring comfort conditions to inhabitants is one of the most essential construction requirements. Being
 440 contemporary raw earth construction a relative new domain, there is still need to design compatible wall assemblies
 441 which could maintain indoors at comfortable levels. In general, thermal comfort is determined by the room's
 442 temperature, humidity and air speed, but there are many additional factors such as activity level, clothing, age,
 443 gender and health status that affect it. Radiant heat (hot surfaces) or radiant heat loss (cold surfaces) are also
 444 important factors for thermal comfort. Optimal microclimatic conditions are deemed to be reached for temperature
 445 range between 19°C and 26°C, and for relative humidity between 40% and 60% [48, 49]. Moreover, relative
 446 humidity of the wall itself is a variable which can have huge impact in the overall thermal behavior of the envelope
 447 and in the durability of the assembly during time. Indeed too high relative humidity inside the CEB wall can result

448 in the development of pathologies or in the decrease of mechanic performances [50]. In the following lines, the
 449 results of numerical simulation run in the reference climate of Paris (France) are presented.
 450 In the following figure 6 it is shown the yearly profile of temperatures variation in the inmost layer of all the
 451 investigated wall assemblies, while on figure 7 the statistical distribution corresponding to the maximum,
 452 minimum and average values for all the tested solutions. It is possible to observe that the largest indoor surface
 453 temperature fluctuation corresponds to the CEB 15 wall assembly which, because of its contained thickness (and
 454 so to its poor thermal capacity) and total absence of thermal insulation layer, is the more prone to outdoor thermal
 455 variations. Indeed, this solution has the largest value dispersion, as it reaches temperature values below 13°C and
 456 above 29°C, indicating poor thermal performance. The increase of the wall thickness to 30 cm and to 45 cm
 457 manage to attain average value which are comprised between 17°C and 24°C for the CEB 30, and 18°C and 23°C
 458 for the CEB 45 solution. It is evident the benefic effects on outdoor temperature mitigation performed by the
 459 increase of CEB wall thickness.
 460 If we focus instead on the insulated solution LH5, LH10 and LH15 and SB5, SB10, SB 15, it is possible to point
 461 out that the variation of average indoor surface temperatures is more contained when compared to the uninsulated
 462 solution. Nevertheless, in LH5 and SB5 scenarios, using only 5 cm thick thermal insulations, the effect of the
 463 thermal insulation is less marked.
 464 In particular, all the simulated maximum indoor surface temperatures are near and all below 26°C during warmer
 465 season, while some differences can be observed in lower temperatures, which are, for the 5 cm-thick insulated
 466 solutions, above 17°C, and for the 10 cm and 15 cm thick insulated solution, above 19°C.
 467 Please note that given the lower thermal conductivity of the SB insulation, the SB insulated solution have a slight
 468 higher thermal performance compared to the LH insulated solutions. Indeed, the performance of the SB 5 and SB
 469 10 solution is almost the same as the LH 10 and LH 15, respectively, with a gain in thermal performance for the
 470 half of the thickness of the insulating layer.



471
 472 *Figure 6. Yearly evolution of indoor surface temperature: temperature profiles*
 473

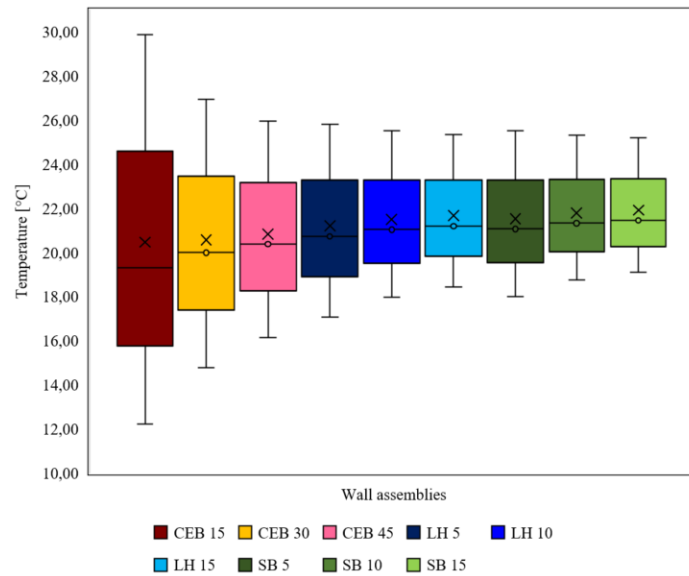


Figure 7. Yearly evolution of indoor surface temperature: statistical distribution

474

475

476 The same effect can be further observed when focusing on envelope's behavior during warmest season. In figure
 477 8 (a, b c) are reported three graph representing the envelope behavior of the three solutions for a warm summer
 478 week (15-21/07/2022). This week is characterized by high outdoor air temperatures which cause high outdoor
 479 surface temperatures (T_{so} , represented by the grey profile in the graphs).

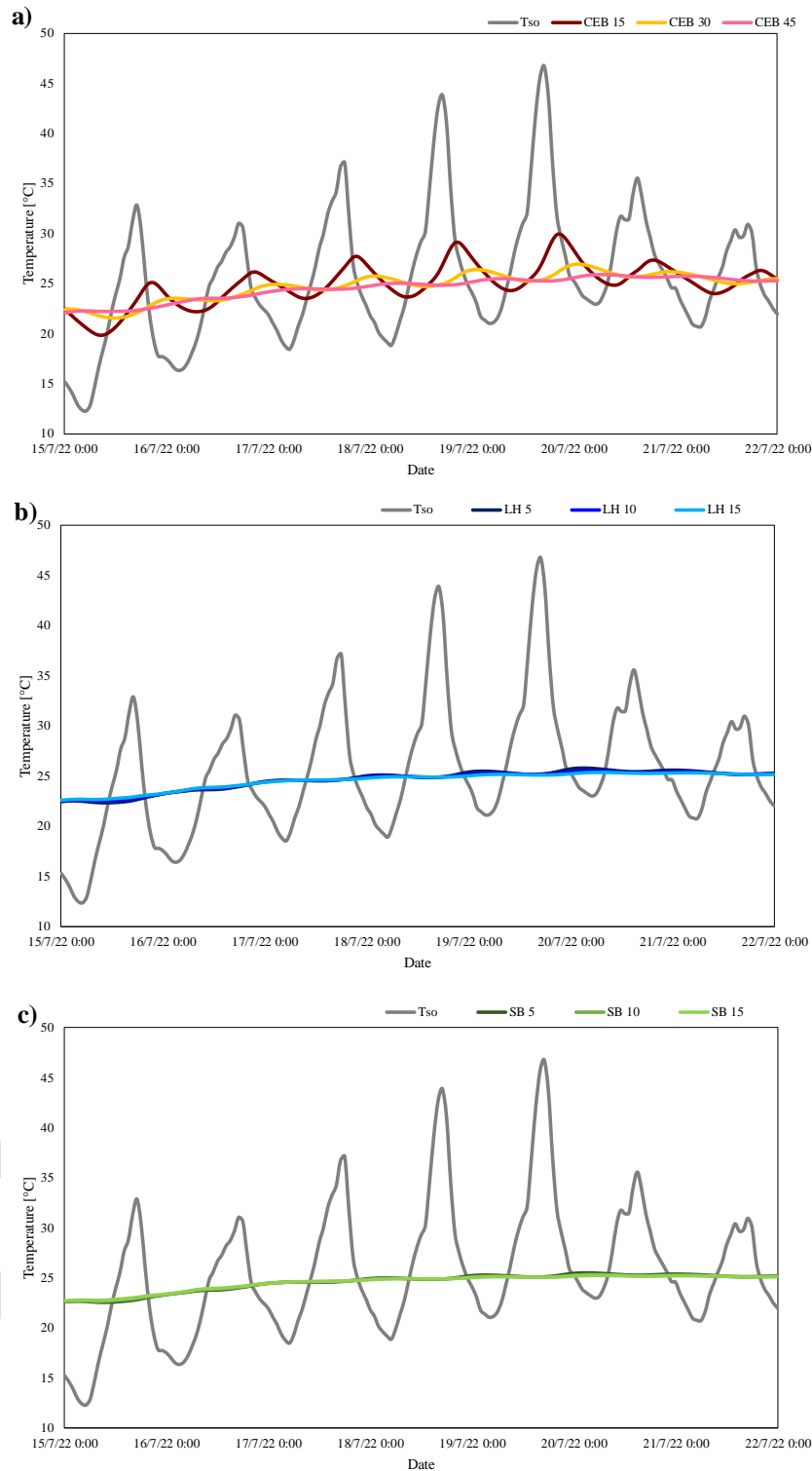
480 If we focus on the warmest week shown in the graph 8a, the influence of the CEB wall thickness on the dynamic
 481 thermal parameters, gives a measure of the dampening and attenuation effect of massive raw earth walls on the
 482 thermal heat wave. Concerning thermal lag, it is equal to 4.1 hours for CEB 15, 8.4 hours for CEB 30 and 14.3
 483 hours for CEB 45 solution. At the same time decrement factor is 0.23 for CEB 15, 0.073 for CEB 30 and 0.033
 484 for CEB 45 solution. Indeed, it is evident that a low thickness is detrimental for the thermal behavior of CEB walls,
 485 walls thicknesses above 30 cm, which correspond to current load-bearing building technologies, reconstitute satisfying
 486 TL and DF.

487 The addition of a 5 cm-thick insulation layer allows an increase of time lag values to 9.5 hours for lime hemp and
 488 to 10.7 hours for sugarcane bagasse, while decrement factor values decrease to 0.02 for LH 5 and to 0.012 for SB
 489 5 solution. Finally, for higher insulations thickness the TL and DF values are near: for 10 cm-thick lime hemp
 490 insulation is 11.7 hours whereas for sugarcane bagasse is 11.2 hours, while DF is 0.011 for the first and 0.006 for
 491 the latter. For 15 cm-thick insulations, TL is 13.5 hours for lime hemp and 12.8 hours for sugarcane bagasse, while
 492 DF is 0.006 for the first and 0.004 for the latter. Calculated values for TL and DF are reported in table 10.

493

Table 10. Time lag and decrement factor of different CEB wall constructions

	CEB 15	CEB 30	CEB 45	LH 5	LH 10	LH 15	SB 5	SB 10	SB 15
TL [h]	4.1	8.4	14.3	9.5	11.7	13.5	10.7	11.2	12.8
DF [-]	0.230	0.073	0.033	0.020	0.011	0.006	0.012	0.006	0.004



494

495 *Figure 8. Outdoor and indoor surface temperature for uninsulated (a), lime hemp insulated (b) and sugarcane bagasse*
 496 *insulated (c) CEB walls of different thickness*

497

4.2.2 *Moisture dependent thermal transmittance of the walls*

498

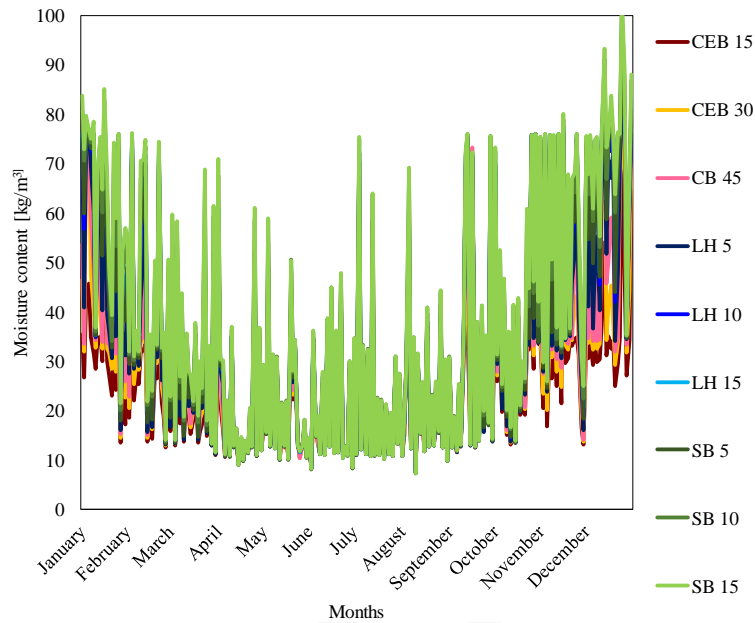
499

500

501

The following figures 9 and 10 show the profiles and the statistical distribution of kilograms of moisture contained for cube meter of wall for the different wall configurations. It is evident that for uninsulated CEB walls of different thickness the amount of water stored is really low, ranging from 16 to 30 kg/m³ for the CEB 15, from 17 to 36 kg/m³ for CEB 30 and from 18 to 40 kg/m³ for CEB 45. The increase of wall thickness cause an increase of

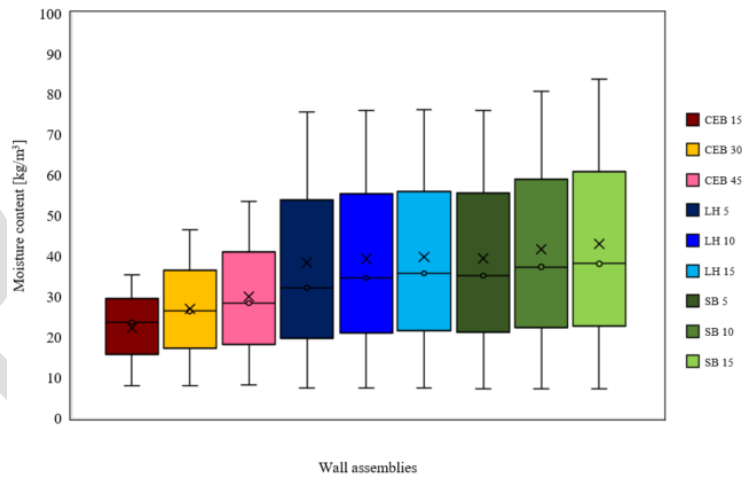
502 moisture stored inside the wall which, as we will see in the second part of this paragraph, worsens the thermal
 503 performance of uninsulated CEB walls.
 504 Different considerations have to be made about moisture contained inside bio-based insulated CEB walls which
 505 store a far higher content of moisture due to the high hygroscopicity of lime hemp and sugarcane bagasse
 506 insulations. Indeed, both LH and SB insulated wall constructions, and in particular for LH 5, LH 10, LH 15 and
 507 SB 5 insulated CEB constructions, the moisture contained inside the wall varies, all over the year, between a
 508 minimum value (during warmest months) of 20 kg/m^3 to a maximum value of 58 kg/m^3 (during coldest months).
 509 Indeed, SB 10 and SB 15 have even higher moisture content, being the highest value around 62 kg/m^3 .



510

511

Figure 9. Yearly evolution of moisture contained in the wall: moisture content profiles



512

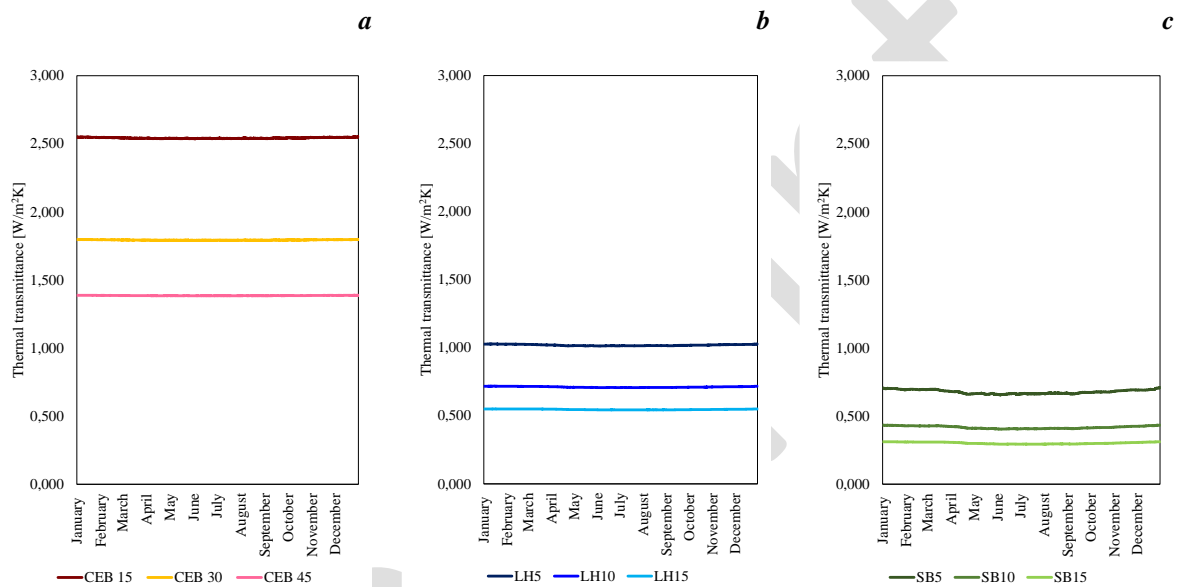
513

Figure 10. Yearly evolution of moisture contained in the wall: statistical distribution

514 Based on results of moisture contained inside the walls and values provided by Delphin software about moisture
 515 dependent thermal conductivity for each layer, it is possible to estimate the moisture dependent U-value for the
 516 nine investigated constructive solutions.

517 From figure 11 is it possible to observe that all along the year, thermal transmittance of uninsulated CEB walls are
 518 quite stable; this result is confirmed in table 11 where the variations between U-value calculated in dry conditions
 519 is compared to moisture dependent U value. Indeed, for CEB 15 solution, U_{dry} is $2.52 \text{ W/m}^2\text{K}$ and average U_{moist}
 520 is $2.54 \text{ W/m}^2\text{K}$ and the increase of U-value in moist condition is 0.69%. Similar values have been found for CEB

521 30 solution for which U_{dry} is 1.78 W/m²K, average U_{moist} is 1.79 W/m²K, with an increase of 0.69% and for CEB
522 45, for which U_{dry} is 1.38 W/m²K and average U_{moist} is 1.39 W/m²K, with an increase of 0.70%.
523 A different behavior is visible for bio-based insulated CEB walls, where the evolution of U-value is worsened by
524 the presence of moisture. In particular, lime hemp insulated solution have a slight worsening of thermal
525 performances compared to uninsulated CEB walls. For instance, LH 5 solution have an increase of U value of
526 4.88% in moist conditions ($U_{dry} = 0.97$ W/m²K, average $U_{moist} = 1.02$ W/m²K). LH 10 solution presents an increase
527 of U value of 6.49% in moist conditions ($U_{dry} = 0.67$ W/m²K, average $U_{moist} = 0.71$ W/m²K). Finally, LH 15
528 solution has and increase of 7.35% of U-value ($U_{dry} = 0.51$ W/m²K, average $U_{moist} = 0.55$ W/m²K).
529 Sugarcane bagasse insulated solution have the highest differences in U-value between dry and moist conditions:
530 SB 5 solution has an increase of U-value of 10.28%, being the $U_{dry} = 0.62$ W/m²K and the average $U_{moist} = 0.68$
531 W/m²K. Higher increases are visible for SB 10 solution, which have a U-value increase of 12.31% ($U_{dry} = 0.37$
532 W/m²K, average $U_{moist} = 0.42$ W/m²K), and for SB 15 solution, for which U-value is increased by the 13.23% (U_{dry}
533 $= 0.27$ W/m²K, average $U_{moist} = 0.30$ W/m²K).



534 Figure 11. Evolution of moisture dependent thermal transmittance all over the year for the investigated CEB walls:
535 uninsulated (a), LH insulated (b) and SB insulated solutions (c)

536 Table 11. Increase of average U-values between moist and dry conditions

	CEB 15	CEB 30	CEB 45	LH 5	LH 10	LH 15	SB 5	SB 10	SB 15
U_{dry} [W/m ² K]	2.52	1.78	1.38	0.97	0.67	0.51	0.62	0.37	0.27
U_{moist} [W/m ² K]	2.54	1.79	1.39	1.02	0.71	0.55	0.68	0.42	0.30
% Increase	0.70	0.70	0.70	4.88	6.49	7.35	10.28	12.31	13.23

537

538 5. Conclusions

539 This work has dealt with the design of bio-based insulated compressed earth blocks walls and with the assessment
540 of their hygrothermal behavior for use in the building vertical envelope. The base wall constructions are composed
541 by compressed earth blocks produced by the French company *Cycle Terre* from the raw earth masses excavated
542 for the *Grand Paris* transport network construction sites.

543 As it is well known, raw earth materials have good thermal inertia but poor thermal insulation properties. For this
544 reason, in this work, several bio-based thermal insulations for compressed earth block walls are proposed. The

545 choice of bio-based thermal insulation is motivated by the comparable moisture storage and transport properties
546 of compressed earth blocks and bio-based insulations as lime hemp and sugarcane bagasse. The comparability of
547 material properties of bio-based and geo-based materials have been confirmed by an in-depth material
548 characterization campaign which has focused on the assessment of dry density, porosity, capillary water
549 absorption, thermal conductivity, specific heat capacity, absorption isotherms and water vapor permeability.
550 On the base of material properties, the impact of bio-based thermal insulations on CEB walls has been studied by
551 means of hygrothermal simulations on Delphin software, which simulates coupled heat and moisture transfers in
552 walls, in the reference climate of Paris (France), classified as a Cfb (marine west coast climate). The simulation
553 study has allowed to compare the impact of CEB wall thickness and bio-based insulation thickness and type on
554 surface wall temperatures, moisture content inside the walls and to assess their impact on dynamic wall behavior
555 and moisture dependent U-value.
556 Concerning the influence of CEB wall thickness on the overall hygrothermal behavior, is possible to infer that thin
557 CEB walls (15 cm) have poor thermal performances, as they lack of both thermal inertia and insulation; moreover,
558 this type of wall does not store a high moisture content. The increase of CEB wall thickness to 30 cm and to 45
559 cm (thicknesses which are in use for loadbearing CEB wall constructions) have a much higher inertial behavior:
560 the time lag is 8.4 hours for the CEB 30 solution and 14.3 for CEB 45 solution, while decrement factor is below
561 0.1. Moisture dependent U-value of these solutions is higher compared to the dry condition U-value but the
562 increase is never above 0.70%. Considering the most common thicknesses used in raw earth construction and the
563 comparable wall behavior between the CEB 30 and CEB 45 solution, the study on the influence of bio-based
564 thermal insulations has been done using 30 cm-thick CEB walls.
565 The influence of bio-based thermal insulation thickness and type on 30 cm-thick CEB walls reveal that the addition
566 of smaller layers of thermal insulations are effective to reduce thermal transfer through walls. As known, dynamic
567 parameters are useful to understand the wall behavior during warmer seasons. Indeed, for lime hemp (LH)
568 insulation, the addition of 5 cm-thick thermal insulation to the CEB 30 construction, give an increase of 13% of
569 time lag (TL) and a reduction of 72.7% of decrement factor (DF). For the same thickness, sugarcane bagasse (SB)
570 manage to attain an increase of TL by the 27% and a reduction of 83.7% of DF. For a 10 cm-thick external
571 insulation, the LH 10 wall has an increase of time lag of 38%, while for the SB 10 wall this increase is limited to
572 33%; at the same time the attained DF reductions are 85.5% and 91.5% for LH 10 and SB 10 solutions. Finally,
573 for the 15 cm-thick wall insulations, the LH 15 solution has an increase of TL of 60% and a decrease of DF by
574 91.2%; furthermore, the SB 15 solution has an increase of TL of 52% and a decrease of DF by 94.7%. Moreover,
575 indoor surface temperatures for all insulated solutions are really near and seasonal minimum and maximum are
576 always comprised between 19°C (during winter) and 23°C (during summer), inside comfort values.
577 It is then possible to infer that in warmer seasons of the analyzed climate, the use of larger insulation thicknesses
578 is not convenient because, the relatively small increase of thermal performance (in comparison with 10-cm thick
579 insulations) could not motivate the extra cost of a thicker insulation. From the simulation study performed in this
580 work, it is found that a 10 cm-thick insulation (both in LH or in SB), is sufficient to ensure a satisfactory wall
581 behavior. Moreover, it appears that in dynamic conditions, more massive thermal insulations as LH performs better
582 compared to lightweight insulation as sugarcane bagasse.
583 The influence of moisture in the evolution of U-value all over the year is more marked for SB insulated solutions
584 than in LH insulated solutions. LH insulation has a poorer thermal performance compared to SB insulation, but
585 when combined with CEB walls, it seems to provide a more stable hygrothermal behavior and a lower quantity of
586 moisture stored inside the wall. For this reason, in the analyzed climate, LH insulated solutions seems to be more
587 safe towards moisture related pathologies inside the walls. Future studies should focus on the lifetime behavior of
588 bio-based insulated raw earth wall constructions, focusing on the risk of moisture related pathologies as
589 development of mold, by comparing experimental data to previsions obtained by means of hygrothermal
590 simulations.

591

592 **CRedit authorship contribution statement**

593 **Giada Giuffrida:** Writing- Original draft preparation, Visualization, Investigation, Software, Data curation,
594 Conceptualization, Methodology. **Hamza Allam:** Writing- Reviewing and Editing, Validation, Supervision,
595 Project administration, Conceptualization, Methodology. **Laurent Ibos:** Writing- Reviewing and Editing,
596 Supervision, Resources, Validation, Conceptualization, Methodology. **Abderrahim Boudenne:** Writing-
597 Reviewing and Editing, Resources, Validation, Conceptualization, Methodology.

598 Acknowledgements

599 The authors want to acknowledge *Cycle Terre* and *Emerwall* Companies for the interest in the research and the
600 continuous technical exchange.

601 References

- 602 1. Giuffrida G, Caponetto R, Nocera F. Hygrothermal Properties of Raw Earth Materials: A Literature Review.
603 Sustainability 2019;11:5342. <https://doi.org/10.3390/su11195342>
- 604 2. Houben H, Guillaud H. *Traité de Construction en Terre*. Éditions Parenthèses 2006 Marseille, France.
- 605 3. Schweiker M, Endres E, Gosslar J, Hack N, Hildebrand L, Creutz M, Klinge A, Kloft H, Knaack U, Mehnert J,
606 Roswag-Klinge E. Ten questions concerning the potential of digital production and new technologies for
607 contemporary earthen constructions. *Building and Environment* 2021;206:108240,
608 <https://doi.org/10.1016/j.buildenv.2021.108240>
- 609 4. Goma M, Jabi W, Soebarto V, Xie YM. Digital manufacturing for earth construction: A critical review. *Journal of*
610 *Cleaner Production* 2022;338:130630, <https://doi.org/10.1016/j.jclepro.2022.130630>
- 611 5. Guide de conception et de construction. *Fabriquer la ville bas carbone avec Cycle Terre*, 2021:01
- 612 6. McGregor F, Heath A, Fodde E, Shea A, Conditions affecting the moisture buffering measurement performed on
613 compressed earth blocks, *Building and Environment* 75 (2014) 11-18
- 614 7. Bruno AW, Gallipoli D, Perlot C, Mendes J, Effect of stabilisation on mechanical properties, moisture buffering and
615 water durability of hypercompacted earth, *Construction and Building Materials* 149 (2017) 733–740
- 616 8. Teixeira ER, Machado G, P. Junior Ad, Guarnier C, Fernandes J, Silva SM, Mateus R. Mechanical and Thermal
617 Performance Characterisation of Compressed Earth Blocks. *Energies*. 2020; 13(11):2978.
- 618 9. Panagiotou R, Kyriakides MA, Illampas R, Ioannou I, An experimental approach for the investigation of the
619 performance of non-stabilized Compressed Earth Blocks (CEBs) against water-mediated weathering, *Journal of*
620 *Cultural Heritage*, 57, 2022, 184-193.
- 621 10. Labiad Y, Meddah A, Beddar M, Physical and mechanical behavior of cement-stabilized compressed
622 earth blocks reinforced by sisal fibers, *Materials Today: Proceedings* 53 (2022) 139–143
- 623 11. Turco C, P. Junior Ad, Teixeira ER, Mateus R, Optimisation of Compressed Earth Blocks (CEBs) using natural
624 origin materials: A systematic literature review, *Construction and Building Materials* 309 (2021) 125140
- 625 12. Ben Mansour M, Jelidi A, Cherif AS, Jabrallah SB, Optimizing thermal and mechanical performance of compressed
626 earth blocks (CEB), *Construction and Building Materials*, 104, 2016, 44-51
- 627 13. Lamrani M, Mansour M, Laaroussi N, Khalfaoui M, Thermal study of clay bricks reinforced by three ecological
628 materials in south of morocco, *Energy Procedia*, 156, 2019, 273-277
- 629 14. Oti JE, Kinuthia JM, Bai J, Design thermal values for unfired clay bricks, *Materials and Design*, 31(1), 2010, 104 -
630 112
- 631 15. Poullain P, Leklou N, Laibi AB, Gomina M, Properties of Compressed Earth Blocks Made of Traditional Materials
632 from Benin, *Revue de Composites et des Materiaux Avancés*, 29(4), 2019, 233 – 241
- 633 16. Amina, L., Joshua, A., Musa, L. (2019). Enhancing the Thermophysical Properties of Rammed Earth by Stabilizing
634 with Corn Husk Ash. In: Sayigh, A. (eds) *Sustainable Building for a Cleaner Environment*. Innovative Renewable
635 Energy. Springer, Cham.
- 636 17. Porter H, Blake J, Kaur NP, Mukherjee A, Rammed earth blocks with improved multifunctional performance,
637 *Cement and Concrete Composites*, 92, 2018, 36-46
- 638 18. Giuffrida, G., Costanzo, V., Nocera, F., Cuomo, M., Caponetto, R. (2023). Natural and Recycled Stabilizers for
639 Rammed Earth Material Optimization. In: Littlewood, J., Howlett, R.J., Jain, L.C. (eds) *Sustainability in Energy and*
640 *Buildings 2022*. SEB 2022. Smart Innovation, Systems and Technologies, vol 336. Springer, Singapore.
- 641 19. Cagnon H, Aubert JE, Coutand M, Magniont C, Hygrothermal properties of earth bricks, *Energy and Buildings* 80
642 (2014) 208–217
- 643 20. Allinson D, Hall M, Hygrothermal analysis of a stabilised rammed earth test building in the UK, *Energy and*
644 *Buildings* 42 (2010) 845–852
- 645 21. Laborel-Préneron A, Magniont C, Aubert JE. Hygrothermal properties of unfired earth bricks: Effect of barley straw,
646 hemp shiv and corn cob addition. *Energy and Buildings*, 2018, 178, 265-278.
- 647 22. Giuffrida G, Detommaso M, Nocera F, Caponetto R. Design Optimisation Strategies for Solid Rammed Earth Walls
648 in Mediterranean Climates. *Energies*. 2021; 14(2):325.
- 649 23. Krayenhoff, M. *Rammed Earth Thermodynamics*. In AA.VV. *Rammed Earth Construction*; Ciancio, D., Beckett,
650 C.T.S., Eds.; Taylor & Francis Group: London, UK, 2015
- 651 24. MacDougall, C.; Dick, K.J.; Krahn, T.J.; Wong, T.; Cook, S.; Allen, M.; Leskien, G. Thermal performance summary
652 of four rammed earth walls in Canadian climates. In AA.VV. *Rammed Earth Construction*; Ciancio & Beckett, Taylor
653 & Francis Group: London, UK, 2015
- 654 25. Goodhew, S.; Griffiths, R. Sustainable earth walls to meet the building regulations. *Energy Build.* 2005, 37, 451–459
- 655 26. Neya I, Yamegueu D, Coulibaly Y, Messan A, Ouedraogo ALSN, Impact of insulation and wall thickness in
656 compressed earth buildings in hot and dry tropical regions, *Journal of Building Engineering*, 33, 2021, 101612

- 657
658
659
660
661
662
663
664
665
666
667
668
669
670
671
672
673
674
675
676
677
678
679
680
681
682
683
684
685
686
687
688
689
690
691
692
693
694
695
696
697
698
699
700
701
702
703
704
705
27. Dong X, Soebarto V, Griffith M, Strategies for reducing heating and cooling loads of uninsulated rammed earth wall houses, *Energy and Buildings* 77 (2014) 323–331
 28. Taylor J, McLeod R, Petrou G, Hopfe C, Mavrogianni A, Castaño-Rosa R, Pelsmakers S, Lomas K, Ten questions concerning residential overheating in Central and Northern Europe, *Building and Environment*, 234, 2023, 110154.
 29. Fiche technique Bloc BTC Cycle Terre: https://www.cycle-terre.eu/wp-content/uploads/2021/04/FT_BTC_201108.pdf
 30. Jami T, Karade SR, Singh LP, A review of the properties of hemp concrete for green building applications, *Journal of Cleaner Production* 239 (2019) 117852
 31. Collet, F., 2017. Hygric and thermal properties of bio-aggregate based building materials. In: Amziane, S., Collet, F. (Eds.), *Bio-aggregates Based Building Materials: State-Of-The-Art Report of the RILEM Technical Committee 236-BBM*. Springer Netherlands, Dordrecht, pp. 125 - 147.
 32. Latif, E., Lawrence, M., Shea, A., Walker, P., 2015. Moisture buffer potential of experimental wall assemblies incorporating formulated hemp-lime. *Build. Environ.* 93, 199-209.
 33. Rode, C., Peuhkuri, R., Time, B., Svennberg, K., Ojanen, T., Mukhopadhyaya, P., Kumaran, M., Dean, S.W., 2007. Moisture buffer value of building materials. *J. ASTM Int. (JAI)* 4 (5), 100369.
 34. Seng B, Magniont C, Lorente S, Characterization of a precast hemp concrete block. Part II: Hygric properties, *Journal of Building Engineering* 24 (2019) 100579
 35. Walker P, Pavia S, Moisture transfer and thermal properties of hemp–lime concretes, *Construction and Building Materials* 64 (2014) 270–276
 36. Ramlee NA, Naveen J, Jawaid M, Potential of oil palm empty fruit bunch (OPEFB) and sugarcane bagasse fibers for thermal insulation application – A review, *Construction and Building Materials* 271 (2021) 121519;
 37. Mehrzad S, Taban E, Soltani P, Samaei SE, Khavanin A, Sugarcane bagasse waste fibers as novel thermal insulation and sound-absorbing materials for application in sustainable buildings, *Building and Environment* 211 (2022) 108753
 38. Standards New Zealand, NZS 4298:2020 Materials and workmanship for earth buildings, 2020
 39. Peruvian Standard, Norma E.080 Diseño y Construcción con Tierra Reforzada, Anexo - Resolución Ministerial N° 121-2017-Vivienda, Ministerio de Vivienda, Construcción y Saneamiento, 2017
 40. Goodhew S, Boutouil M, Streiff F, Le Guern M, Carfrae J, Fox M, Improving the thermal performance of earthen walls to satisfy current building regulations, *Energy & Buildings* 240 (2021) 110873
 41. Caponetto R, Cuomo M, Detommaso M, Giuffrida G, Presti AL, Nocera F. Performance Assessment of Giant Reed-Based Building Components. *Sustainability*. 2023; 15(3):2114.
 42. Idder A, Hamouine A, Labbaci B, Abdeldjebar R, The Porosity of Stabilized Earth Blocks with the Addition Plant Fibers of the Date Palm, *Civil Engineering Journal* 6(3), 2020, 478 – 494
 43. Costi de Castrillo M, Ioannou I, Philokyprou M, Reproduction of traditional adobes using varying percentage contents of straw and sawdust, *Construction and Building Materials* 294 (2021) 123516
 44. Eires R, Camoes A, Jalali S, Enhancing water resistance of earthen buildings with quicklime and oil, *Journal of Cleaner Production* 142 (2017) 3281-3292
 45. Bruno AW, Gallipoli D, Perlot C, Kallel H, Thermal performance of fired and unfired earth bricks walls, *Journal of Building Engineering* 28 (2020) 101017
 46. Chennouf N, Agoudjil B, Boudenne A, Benzarti K, Bouras F, Hygrothermal characterization of a new bio-based construction material: Concrete reinforced with date palm fibers, *Construction and Building Materials* 192 (2018) 348–356
 47. Urso A, Costanzo V, Nocera F, Evola G, Moisture-Related Risks in Wood-Based Retrofit Solutions in a Mediterranean Climate: Design Recommendations, *Sustainability*, 2022, 14, 14706
 48. Kunkel S, Kontonasiou E, Indoor air quality, thermal comfort and daylight policies on the way to nZEB – status of selected MS and future policy recommendations, *ECEE Summer Study Proceedings*, 2015, 1261-1270
 49. Detommaso M, Gagliano A, Marletta L, Nocera F. Sustainable Urban Greening and Cooling Strategies for Thermal Comfort at Pedestrian Level. *Sustainability*. 2021; 13(6):3138
 50. Vegas F, Mileto C, Proyecto COREMANS: Criterios de intervención en la arquitectura de tierra, Ministerio de Educación, Cultura y Deporte, 2017, 030-17-184-9